

## EXPERIMENTAL INVESTIGATION ON THE ACOUSTIC CHARACTERISTICS OF LOX/CH<sub>4</sub> FLAME

L. Hong<sup>1</sup>, A. Fusetti<sup>2</sup>, M. De Rosa<sup>3</sup>, and M. Oswald<sup>4</sup>

<sup>1</sup>Northwestern Polytechnical University, China, hongliu2020@yahoo.com.cn

<sup>2</sup>Space Propulsion Institute, DLR, Germany, afuso@tiscali.it

<sup>3</sup>Space Propulsion Institute, DLR, Germany, marco.derosa@dlr.de

<sup>4</sup>Space Propulsion Institute, DLR, Germany, Michael.Oswald@dlr.de

**ABSTRACT** Experimental results of a test campaign on the interaction of a cryogenic LOX/CH<sub>4</sub> spray flame with an acoustic excitation are given in the paper. Liquid oxygen and gaseous methane are injected with a shear coaxial injector. The flame was visualized by detecting the OH emission with a frame rate up to 27 kHz. Simultaneously shadowgraph images were also recorded to visualize the flow field. The flame behavior under different chamber pressure and different mixture ratio is compared. A pressure modulator device was used to excite acoustic pressure oscillations in the combustion chamber. The first transversal and the first longitudinal combustion chamber mode could be excited during hot fire tests. Two strong low frequency instabilities were found under high frequency external disturbance. A lifted flame has been observed under the experimental conditions and the characteristic of the lift-off distance is discussed in the current paper.

**Keywords:** Acoustic Characteristics, Methane, Combustion Instability, Flame Front Position, Liquid Jet

### 1. INTRODUCTION

Combustion instability results from a coupling of combustion with the fluid dynamics of a system. The coupling feeds energy from the combustion process into oscillatory pressure fluctuations. If damping processes in the combustor are not efficient, the amplitude of these oscillations can increase to levels that impair rocket engine performance seriously. Combustion instability problems were encountered in almost every developing project of large scale liquid rocket engines. During the development of F-1 engine, nearly 2000 hot tests among 3200 full scale hot tests were used to treat high frequency combustion instability [1]. Up to now, the instability problem can only be treated in a trial and error way due to poor understanding of its mechanism. Therefore it is a time consuming and costly issue.

Combustion instability is a very complicated process. The characteristics of liquid drops, including vaporization rate, size distribution and secondary atomization, are known to play a very important role in combustion instability. In an oscillating pressure field the pressure dependent vaporization rate of liquid drops can trigger combustion instability in certain frequency ranges. The oscillation of the velocity in an instable combustion field can cause big drops in the liquid jet to break into small drops, which increases the local energy release and become a potential driving force to combustion instability.

The process of breakup, atomization and vaporization of liquid oxygen and subsequent mixing with the gaseous phase are generally described by non-dimensional numbers, characterizing the propellant flow condition at the injector exit. The momentum flux

$$J = \frac{\rho_g v_g^2}{\rho_l v_l^2} \quad (1)$$

has been shown to control the intact core length in cold flow tests [2,3]. The We number

$$We = \frac{\rho_g (v_g - v_l)^2 d_l}{\sigma} \quad (2)$$

represents the ratio between the aerodynamic forces and the surface tension force and is used to classify the atomization process [4]. We is a key parameter for secondary atomization. Another important parameter is the injection velocity ratio of gas over liquid, as defined by:

$$RV = \frac{v_g}{v_l} \quad (3)$$

However, to describe analytically the process of the jet formation, breakup, atomization, heat exchange and recirculation zone is very difficult due to the complexity of the liquid jet atomization process and the interaction of the flow dynamics with combustion. Experiments at as near as possible representative conditions, i.e. original fluids, reactive sprays, and high pressure are required that allow to characterize the atomization and combustion processes.

The current testing campaign is part of a testing series on the spray and combustion of LOX and methane. In previous tests, a difference between LOX/hydrogen and LOX/methane spray flames under similar injection conditions was found [5]. The flames of a LOX/H<sub>2</sub> spray flame are anchored at the exit of the injector, however the flame of LOX/CH<sub>4</sub>-flames were observed to be lifted at most of the test conditions.

Lifted flames are expected to be sensitive to flow fluctuations which is a potential coupling mechanism leading to combustion instability. Therefore the present test campaign was performed to get a better understanding of the interaction of acoustics with LOX/CH<sub>4</sub> spray flame anchoring and combustion. Pressure oscillations at eigenfrequencies of the combustor are induced and the response of the flame and the flow is analyzed. Two types of excitations have been applied: in the first case the velocity vectors of the excited acoustic waves were perpendicular to the spray axis (transversal combustor modes), in the second case they were parallel to the spray

axis (longitudinal combustor modes).

## 2. EXPERIMENTAL SETUP

The experiments have been performed at the micro-combustor test facility at DLR Lampoldshausen. Details concerning the micro-combustor can be found in [6]. The combustor was equipped with a single coaxial injector. The liquid oxygen was injected through the central post, and the methane gas was injected through the coaxial annulus. The thickness of the LOX post was fixed at 0.4mm. The diameter of the post and the annulus can be changed according to different test conditions. In the tests, two different sizes of injectors and nozzles were used, which are shown in detail in table 1.

Table 1: Geometry parameters

<i>excited mode</i>	<i>LOX post (mm)</i>	<i>Annulus (mm)</i>	<i>Main nozzle (mm)</i>	<i>Secondary nozzle (mm)</i>
1L mode	Ø1.2	Ø4.9	Ø12 Ø17	Ø3
	Ø1.6	Ø5.7		
1T mode	Ø1.2	Ø4.9	Ø12 Ø17	1.9x4
	Ø1.6	Ø5.7		

Pressure oscillations in the combustion chamber at specific frequencies have been induced by a device similar to that used by Lecourt and Foucauld [7]. A secondary nozzle was mounted with an area of about 3.1% and 6.5% of the Ø12mm and Ø17mm main nozzle respectively. A siren wheel modulated the gas flow through the secondary nozzle. The exit of the secondary nozzle is open and blocked intermittently by these teeth. The excitation frequency can be controlled by the angular frequency of the wheel and the number of teeth on its circumference. With 100 teeth the maximum excitation frequency was 10 kHz. With the frequency adjusted to an eigenfrequency of the combustor a standing wave is excited with a pressure anti-node at the location of the secondary nozzle. Two different secondary nozzles have been used for the excitation of transversal and longitudinal modes. For transversal modes the secondary nozzle has been mounted in the bottom wall of the combustor (see Fig. 1), thus the induced acoustic velocity field was perpendicular the LOX-jet axis. For longitudinal modes the secondary nozzle has been mounted at the end of the combustor (see Fig. 2), thus the induced acoustic velocity field was parallel to the LOX-jet axis.

Before ignition, the angular frequency of the wheel was increased to a certain level and then kept constant until ignition. During the two seconds of test duration, the wheel is accelerated again to cover the frequency range of interest.

Two optical quartz windows were mounted on the two long vertical sides of the combustion chamber to give access for optical diagnostics (Fig.2). In the upper and

lower walls of the combustor dynamic pressure sensors were mounted. Resonance volumes in these walls have been tuned to adjust the transversal eigenfrequency of the system to the frequency range of the siren wheel.

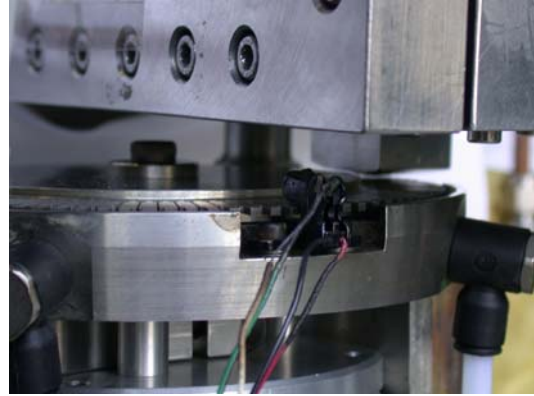


Fig.1 Mounting Position of the pressure modulator device for transversal mode test

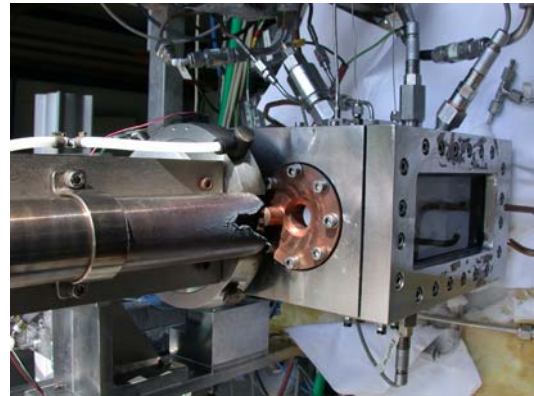


Fig.2 Mounting Position of the \*pressure modulator device for longitudinal mode test

To compare the influence of the pressure on instability in the combustion chamber, four different chamber pressures, 0.15MPa, 0.2MPa, 0.3MPa and 0.4MPa, were tested. Three different mixture ratios of oxygen to methane, 2.5, 3.4 and 4, were also chosen to compare the influence of mixture ratios.

The optic diagnostic system consists in a high resolution CCD camera for shadowgraph (Kodak FLOWMASTER 2k) images and a high speed intensified CCD camera (Photron I2) fitted with a Nikkor UV objective for recording the OH radical emission. The shadowgraph system is backlit by a nanolite, with 18 ns flash duration. This very short flash duration allows to “freeze” the flow. The high resolution is paid in terms of low acquisition rate (4 kHz). The high speed UV camera acquisition rate sets at 27 kHz. This allows us to visualize and to analyze high frequency oscillation of flames. The UV camera was focused on the area near injector face plate to get a better visualization of flame front.

## 3. EXPERIMENTAL RESULTS

### 3.1 Tests with transversal acoustic excitation

In rocket combustion the transversal modes are most prominent for triggering combustion instabilities. By means of the commercial code Flex PDE for numerical solution of partial differential equations, the eigenfrequency of the

1T mode is predicted to be about 9.2kHz for the micro-combustor, and the eigenfrequencies of higher transversal modes are much higher than 10kHz, beyond the range accessible with the of pressure modulator device. Therefore, only the 1T mode was tested.

For injector configuration I,  $d_0=1.2\text{mm}$ ,  $d_2=4.9\text{mm}$ , tests were performed at  $P_c=0.2\text{MPa}$ ,  $0.3\text{MPa}$  and  $0.4\text{MPa}$ . The pressure oscillating with 1T eigenfrequency was found which can be seen from Fig. 3. The frequency of 1T mode is 9121Hz. The peak to peak ratio of pressure fluctuation  $\Delta p$  to the mean chamber pressure  $\Delta p/\bar{p}_c=9\%$ .

For injector configuration II,  $d_0=1.6\text{mm}$ ,  $d_2=5.7\text{mm}$ , shadowgraph images of two pairs of tests were shown in Fig.4. The time between images is 0.35ms. The first three rows refer to two tests with and without excitation at relatively higher J, in which images for “off resonance” and for “on resonance” are taken from different time interval of the same test. The last two rows refer to two tests at relatively lower J.

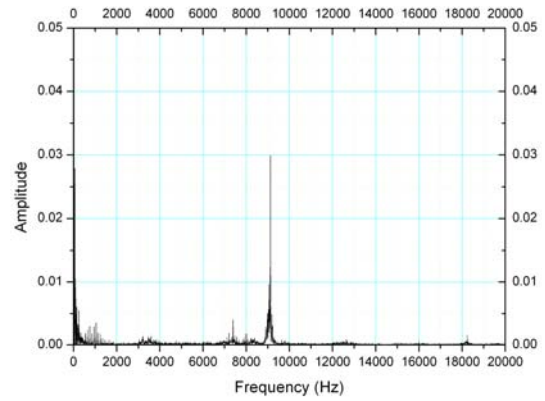


Fig.3 FFT result of dynamic pressures in the combustor with injector configuration I

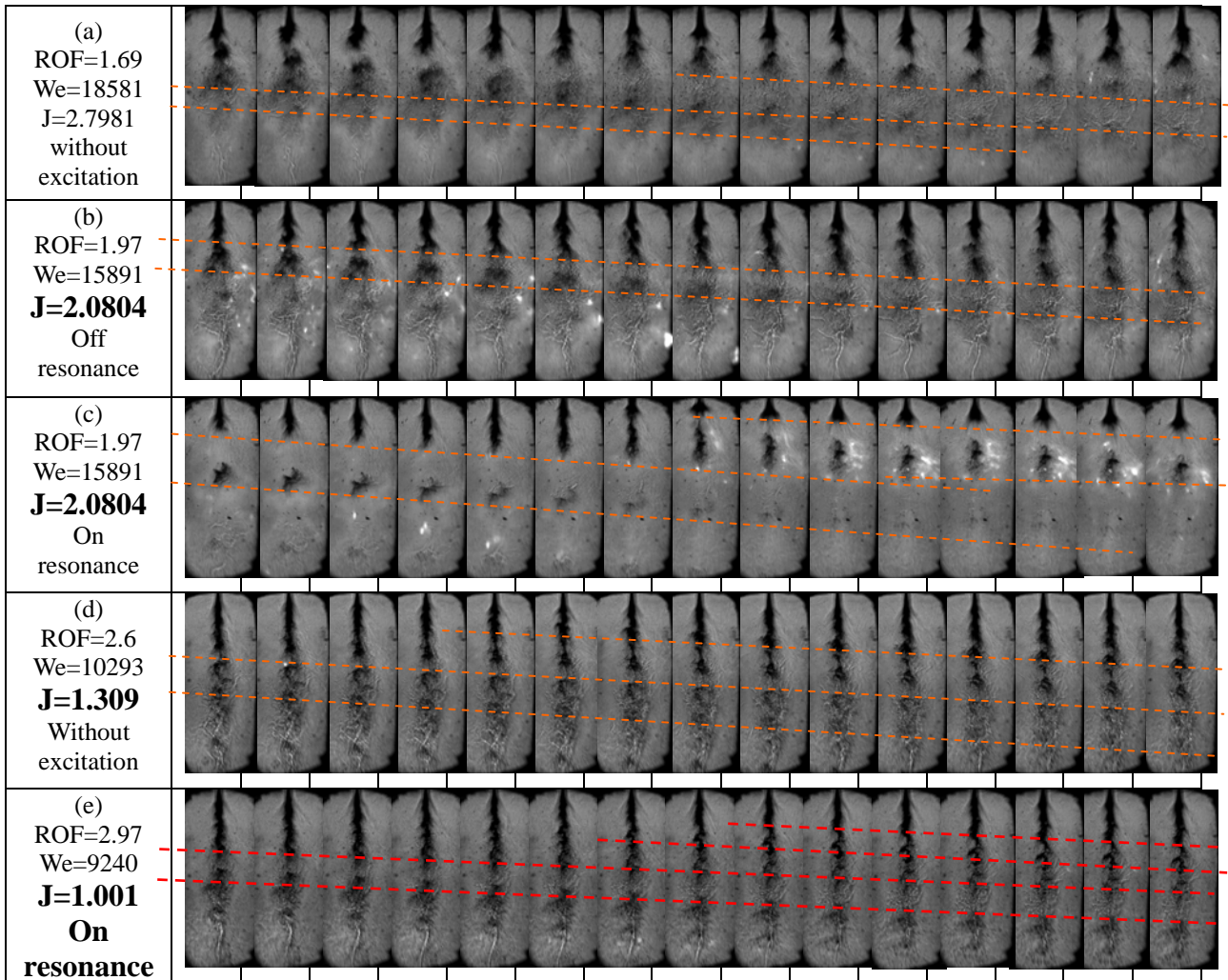


Fig.4 Comparison of spray behavior with and without excitation

It's clear from Fig.4 that at higher J the stronger aerodynamic force from the CH<sub>4</sub> co-flow breaks the jet earlier and hence the intact length is shorter, which conforms the empirical formula for predicting intact core length given by Villermaux [8] in tendency. The broken part of liquid oxygen is surrounded by hot gas, atomizing and burning while moving downstream. In this case the chemical reactive

zone is nearer to the injector face. The pressure rise resulted from fast burning of broken liquid oxygen drop pushes jet end back and forms the ‘brush-like’ atomization as shown in the first row of Fig.4. At the end of the potential liquid oxygen core, the jet breaks into liquid filament, and then into big and small drops.

The above different processes of atomization at higher J

make the response of jet to external disturbance different. It can be seen from the row (c) in Fig.4 that at higher J the pressure oscillation in combustion chamber is enhanced on resonance, which makes the liquid oxygen injected in an instable way. The broken part of liquid oxygen burned much faster and the chemical reaction is nearer to the injector face. Whereas, the liquid oxygen jet at lower J is broken at the end of it by transversal external disturbance into filament, the broken part moves downstream, atomizing and burning relatively near the nozzle. The jet is stable, but it can be seen from the UV images clearly that the gas around the jet waves periodically in transversal direction.

The slope of red dashed lines in Fig.4 indicates the convection speed of LOX. It is from 1.5 to 2 times of the injection speed of LOX. Under the action of high speed CH4 co-flow, the moving of LOX is accelerated.

If correlating the last seven images in the row (c) with dynamic pressure, these images were recorded in the same time interval with the maximum pressure peak marked by a black ellipse, shown in Fig. 5. It's clear that more and more drops are stripped from LOX jet and burned with the increasing transversal velocity field caused by pressure oscillation in resonance zone, and the chamber pressure is hence increased. With the increasing of chamber pressure, the pressure difference across injector becomes smaller and smaller, at the same time the injection is lowered down, as shown in row (c) of Fig. 4.

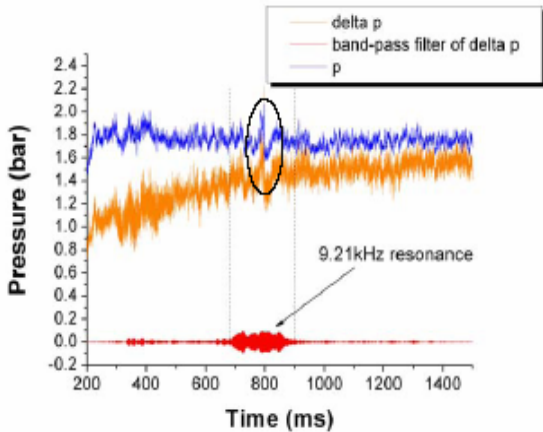


Fig.5 Chamber pressure for the test shown in row (c) of Fig. 4

From Fig. 4, it seems exist a periodic injection at medium frequency around 500~ 1000Hz. Checking the time period of the broken part of LOX from the moment broken to completely burned out or exit the combustor, it can be found that the broken LOX part existed in the combustor for 23 images, i.e. 5.5 ms. the frequency referring to this time is about 182Hz. Filtering the dynamic pressure around 90 Hz, 180 Hz and 9.21 kHz shown in Fig. 6, very weak LF oscillation with frequency around 90Hz and 180Hz were also found. Fig 6 shows a resonant enhancement of the amplitude from about 750ms to 850ms, i.e. during 100ms. With a ramp of 400Hz/s this corresponds to a resonance width of about 40 Hz.

The contribution of 1T oscillation to the pressure fluctuation  $\Delta p$  for the test described by row (b) and (c) in Fig. 4 reaches 11% of the mean chamber pressure, which is a little higher than 10.5% for the test at lower J as shown in

row (e) of Fig.4. From the viewpoint of maximum pressure oscillation peak referring to the frequency of interest, the response intensity to excitation is similar for both cases with different J and mixture ratio.

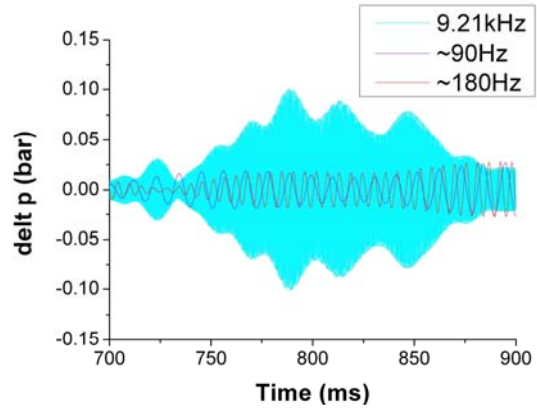


Fig. 6 Band-pass filtering result of dynamic pressure for test shown in row (c) of Fig.5

The flame front position is also of great interest of the current test campaign. Treating the UV images with a proper threshold value, the edge of each flame and then the flame front position relative to injector face can be determined.

For tests described by the first three rows, the comparison of flame front position is plotted as a function of time in Fig. 7. No significant difference is found for the two tests with or without transversal excitation.

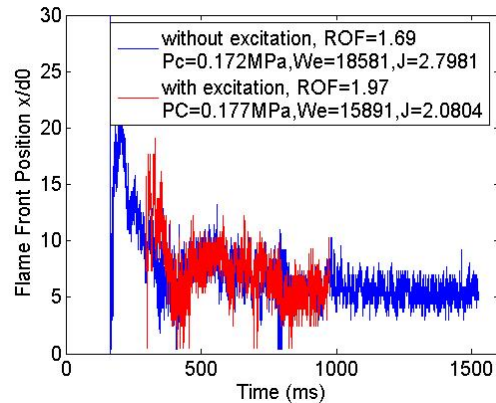


Fig.7 Comparison of flame front position with or without transversal excitation

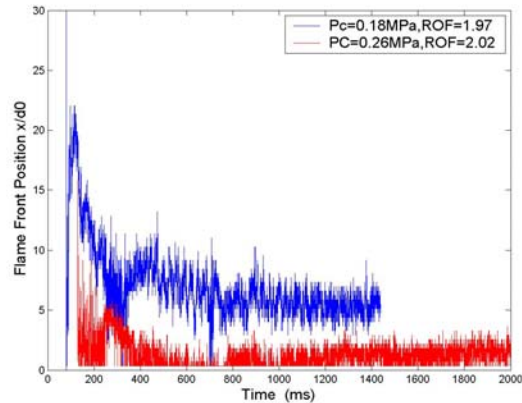


Fig.8 Comparison of flame front position at different chamber pressure and oxygen lean condition with 1T excitation ( $d_0= 1.6$  mm,  $d_2= 5.6$  mm)

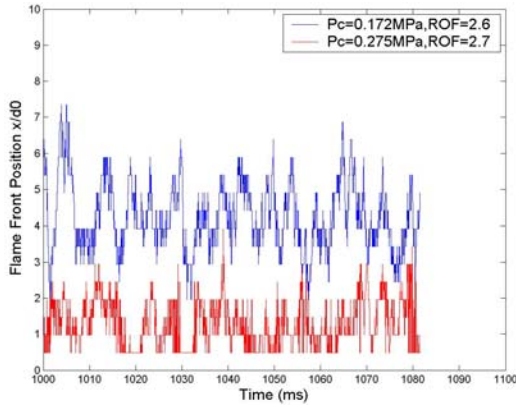


Fig.9 Comparison of flame front position at different chamber pressure without excitation (  $d_0 = 1.6 \text{ mm}$ ,  $d_2 = 5.6 \text{ mm}$  )

The influence of the chamber pressure  $P_c$  on the flame front position was compared in Fig.8 - 10. It's clear that higher pressure is always beneficial for flame anchoring no matter with or without excitation in the range of mixture ratios tested. However, if the flame front positions of all tests at stable state are plotted as a function of chamber pressure  $P_c$ , the dependence of flame front position on  $P_c$  is not so clear. The causes affecting the flame front position are very complicate. Here only three pairs of tests are compared,

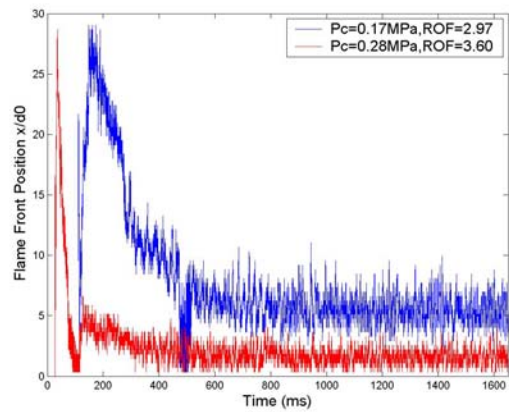
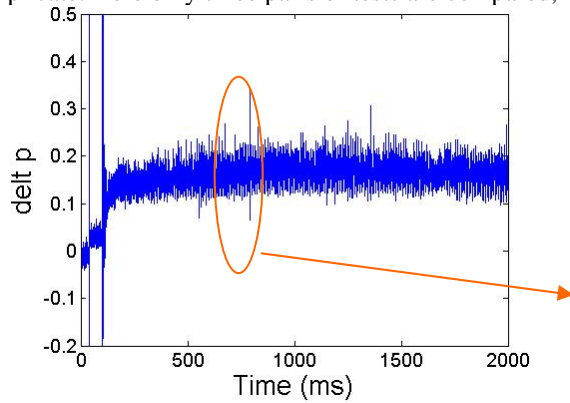


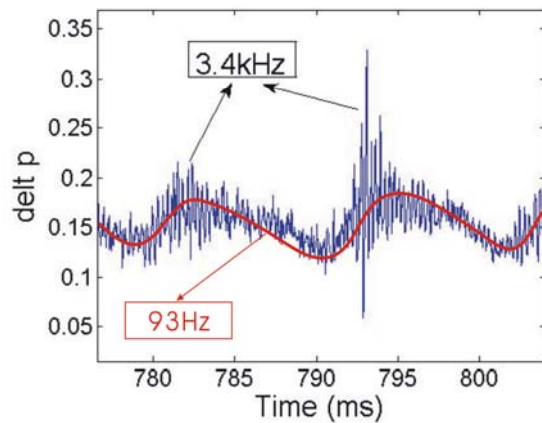
Fig.10 Comparison of flame front position at different chamber pressure and oxygen rich condition with transversal excitation (  $d_0 = 1.6 \text{ mm}$ ,  $d_2 = 5.6 \text{ mm}$  )

### 3.2 Tests for 1L modes triggering

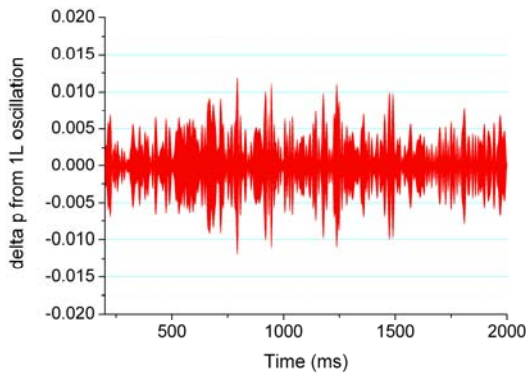
The eigenfrequency of 1L mode predicted by Flex PDE code is 3.4 kHz. Therefore the ramping of the gas modulator device was set between 2.8 kHz – 4kHz for all the tests with 1L excitation.



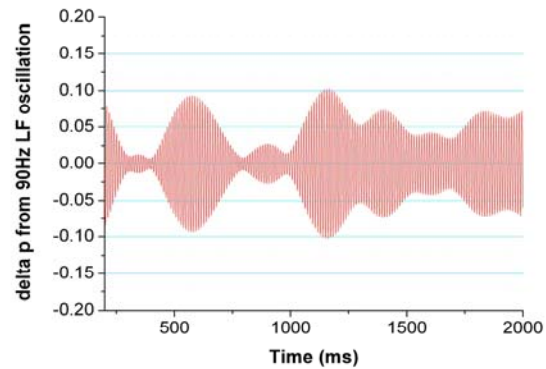
(a) Dynamic pressure



(b) Expanding of dynamic pressure



(c) Band pass filtering of dynamic pressure near 1L eigenfrequency of 3.4kHz



(d) Band pass filtering of dynamic pressure near 93Hz

Fig 11 Comparison of Shadowgraph and OH emission images for 1L test at the condition of “on resonance” and “off resonance ( $d_0=1.6, d_2=5.7, P_c=0.244\text{MPa}$ ,  $ROF=2.99, We=12915, J=0.7066$ )

In the test campaign, several tests for 1L mode triggering with different injectors, different chamber pressures and different mixture ratios were performed. Fig.11 shows a test with strong low frequency oscillation which will be discussed in the next section. After expanding the dynamic pressure distribution curve at the time near the maximum peak, it can be seen clearly that a high frequency oscillation of 3.4kHz is coupled with 93Hz LF oscillation. At each LF maximum pressure there is a HF maximum pressure. After carefully filtering the dynamic pressure, contributions of 1L oscillation and 93Hz LF oscillation to dynamic pressure can be obtained in Fig. 11 (b) and (c). The 1L oscillation contributes only 1% of mean chamber pressure, whereas 93 Hz LF oscillation contributes 8.2%. The FFT magnitude of 1L oscillation is also very small. Therefore the resonance of 1L eigenmode is very weak.

### 3.3 Discussion on Low frequency oscillation

Among tests for transversal and longitude eigenmodes triggering, there are two tests in which strong low frequency oscillation was found, see Fig.12. One is for 1T mode triggering. A strong  $((\Delta p/\bar{p}_c)_{93Hz} = 35\%)$  low frequency instability was found accompanying with the 1T resonance. Two instability frequencies, 93Hz and 180Hz, in the combustion chamber and fuel dome were recorded, see Fig.13.

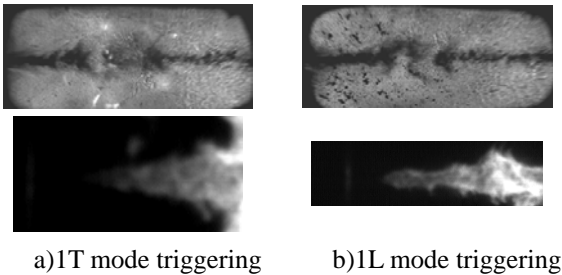


Fig.12 Shadowgraph images and OH emission images of low frequency instability

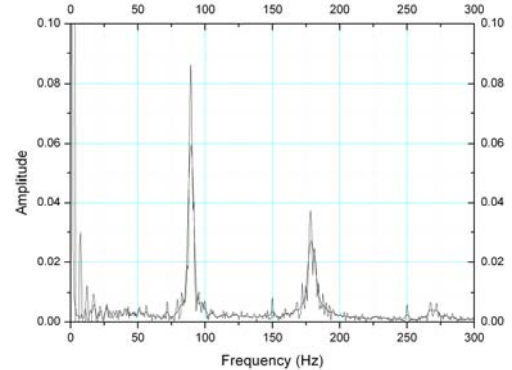
The other LF-Instability has been observed for 1L mode triggering. The instability frequencies are the same as the previous one, but the pressure oscillation caused is a little smaller  $((\Delta p/\bar{p}_c)_{93Hz} = 8.2\%)$  than the case for 1T mode triggering.

As mentioned in sector 3.2, a coupling phenomenon of 1L oscillation with 93Hz LF oscillation is found, whereas no coupling of 1T with LF oscillation can be found in the 1T triggering case.

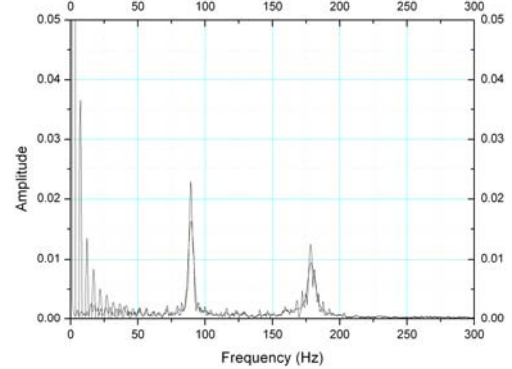
The two peaks found in the Fourier spectrum at 93 Hz and 180 Hz. The 180 Hz peak is probably just an overtone of the 93 Hz-peak. The reason for occurring of low frequency instability at very high triggering frequency is not clear. In the fuel feed system, no such a characteristic length can be found to match the low instability frequencies, because there is a sonic nozzle about 15cm upstream of the injector face plate.

Fig.14 shows the stability boundary for low frequency oscillation, in which “with LF” and “without LF” represents

the tests in which the low frequency oscillation had been found or not respectively. The two solid red circles represent the two tests with strong low frequency instability mentioned above. From Fig.14, it’s clear that the low frequency oscillation is sensitive to the external disturbance inputted from transversal direction or axial direction at medium We number (ranging from 1200 to 1400) and medium momentum ratio J (ranging from 0.5 to 1.6). Outside this range of We and J, no obvious low frequency oscillation was found, even for the case with strong high frequency instability.



(a) LF instability in combustion chamber



(b) LF instability in fuel dome  
Fig.13 Low frequency instability

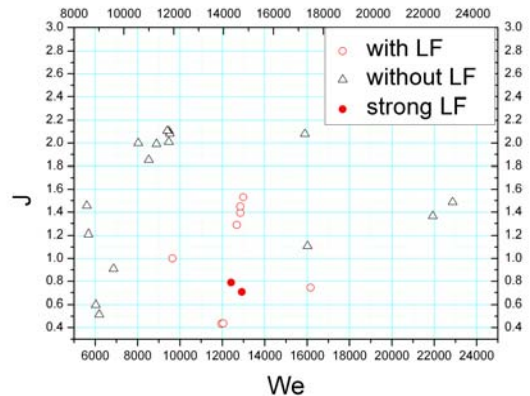


Fig.14 Stability boundary for Low frequency

Fig.15 gives the comparison of flame front position of the two tests mentioned above, which has strong low frequency oscillation. It shows that the axial triggering disturbance can cause a little bigger lift off distance of flame than the transversal triggering. Low frequency oscillation

favors large axial oscillation of flame front. This also can be seen clearly from Fig. 16 that low frequency oscillation always cause flame front oscillating in a large axial range. With or without excitation has no obvious influence on flame front position.

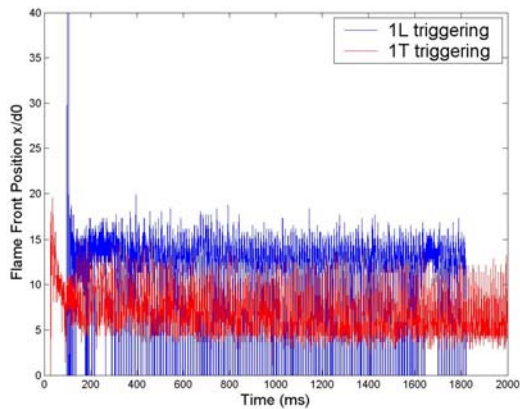


Fig.15 The comparison of flame front position between 1L and 1T triggering with LF oscillation

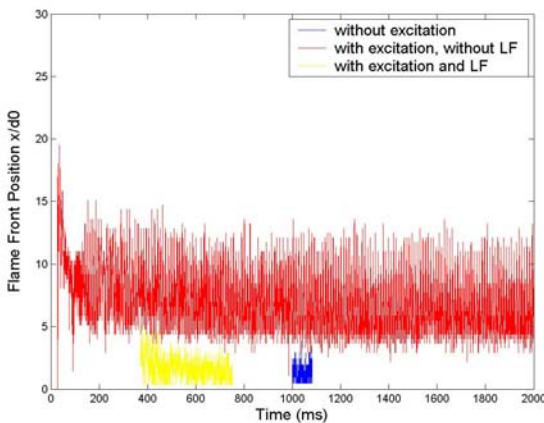


Fig.16 The comparison of flame front position with or without LF oscillation

#### 4. CONCLUSION

The test campaign for investigating the acoustic characteristics of LOX/Methane flames had been successfully conducted at M3 test bench in DLR-Lampoldshausen. The results are summarized here:

- (1) The 1T modes were successfully triggered with pressure modulator device at different mixture ratio and different

chamber pressure.

- (2) The characteristic of spray and its response to external excitation was found. The spray pattern changes significantly on resonance.
- (3) In 1L eigenmode triggering test, the coupling phenomena of 1L high frequency oscillation with LF oscillation was found.
- (4) At the medium We number (ranging from 1200 to 1400) and the medium momentum ratio (ranging from 0.5 to 1.6), the low frequency oscillation is sensitive to external disturbance, no matter it is inputted from transversal direction or longitude direction.
- (5) At the same condition, the increase of the chamber pressure is beneficial for flame anchoring. 1T excitation has no obvious influence on flame front position. When lower frequency oscillation happens, the flame front undergoes a large axial oscillation.

#### 5. REFERENCE

1. "Liquid Rocket Engine Combustion Instability", Edited by Vigor Yang and William Anderson, Vol. 169, Progress in Astronautics and Aeronautics, July, 1995.
2. Lasheras, J.C.; Villermaux, E.; Hopfinger, E.J., "Break-up and atomization of a round water jet by a high-speed annular air jet", Journal of Fluid Mechanics, Vol. 357, pp- 351-379, 1998
3. Davis, D.W.; Chehroudi, B., "Shear-coaxial jets from a rocket-like injector in a transverse acoustic field at high pressures", AIAA 2006-0758, 44th Aerospace Sciences Meeting, Reno, NV, 2006
4. Farago, Z.; Chigier, N., "Morphological classification of disintegration of round jets in a coaxial air stream", Atomization and Sprays, Vol. 2, No. 2, 1992, pp. 137-153
5. F. Cuoco, B. Yang, M. Oswald, "Experimental Investigation of LOx/H2 and LOx/CH4 Sprays and Flames", 24th International Symposium on Space Technology and Science, May 30 – June 6 , 2004, Miyzaki, Japan, ITS 2004-a-04
6. Gurliat, O.; Schmidt, V.; Haidn, O.H.; Oswald, M., "Ignition of Cryogenic H2/LOX Sprays", Aerospace Science and Technology, Vol. 7, 2003, pp. 517-531
7. R. Lecourt, R. Foucaud, "Experiments on stability of liquid propellant rocket motors", AIAA paper 87-1772.
8. Villermaux E., Mixing and Spray Formation in Coaxial Jets, Journal of Propulsion and Power, Vol. 14, No. 5, 1998.